Computational Methods for Differential Equations
http://cmde.tabrizu.ac.ir
Vol. 6, No. 3, 2018, pp. 295-311

A method based on the meshless approach for singularly perturbed differential-difference equations with Boundary layers

Fahimeh Akhavan Ghassabzade
Department of Applied Mathematics, Faculty of Mathematical Sciences,
Ferdowsi University of Mashhad, Mashhad, Iran.
E-mail: akhavan_gh@yahoo.com

Jafar Saberi-Nadjafi*
Department of Applied Mathematics, Faculty of Mathematical Sciences,
Ferdowsi University of Mashhad, Mashhad, Iran.
E-mail: najafi141@gmail.com

Ali Reza Soheili
Department of Applied Mathematics, Faculty of Mathematical Sciences,
Ferdowsi University of Mashhad, Mashhad, Iran.
E-mail: soheili@um.ac.ir

Abstract In this paper, an effective procedure based on coordinate stretching and radial basis functions (RBFs) collocation method is applied to solve singularly perturbed differential-difference equations with layer behavior. It is well known that if the boundary layer is very small, for good resolution of the numerical solution at least one of the collocation points must lie in the boundary layer. In fact, a set of uniform centers is distributed in the computational domain, and then coordinate stretching based transform is used to move the centers, to the region with high gradients. In addition to the integrated multiquadric (MQ) collocation method is applied to solve the transformed equation. The effectiveness of our method is demonstrated on several examples with boundary layer in both cases, i.e., boundary layer on the left side as well as the right side.

Keywords. Differential-difference equation, Boundary layer, Multiquadric collocation method, Radial basis function.

2010 Mathematics Subject Classification. 34K10, 34A36.

1. Introduction

Singularly perturbed differential-difference equations have arisen in many fields such as in the study of an optically bistable device [1] and in a variety of models for physiological processes or diseases [13, 24]. Such type of problems also appear in the description of the so-called human pupil light reflex [12] and variational problems in control theory [6], where they provide the best and in many cases the only realistic simulation of the observed phenomena. Boundary value problems (BVPs) involving

Received: 19 July 2017 ; Accepted: 28 May 2018.
∗ Corresponding author.

differential-difference equations also arise in mathematical models of neuronal variability [21]. The theory and numerical solution of singularly perturbed differential-difference equations are still at the initial stage. In [20] Kolloju Phaneendra et al. presented a numerical method to solve boundary value problems for singularly perturbed differential difference equations with negative shift. Let us consider the following boundary-value problem for a class of singularly perturbed differential-difference equations

$$\varepsilon y''(x) + p(x)y'(x-\delta) + q(x)y(x) = f(x), \ \ \forall x \in (0,1), \tag{1.1}$$

$$y(x) = \omega(x) \ \ \text{on} \ \ -\delta \leq x \leq 0, \tag{1.2}$$

$$y(1) = \gamma, \tag{1.3}$$

where ε is a small parameter, $0 < \varepsilon \ll 1$ and δ is also small shifting parameter, $p(x)$, $q(x)$ and $f(x)$ are smooth functions and γ is a constant. If a function $y(x)$ is a smooth solution to the problem (1.1)-(1.3), then it must satisfy (1.1)-(1.3), be continuous on [0,1] and be continuously differentiable on (0,1).

The boundary value problems for the above class of singularly perturbed differential difference equations contain delay only in the first-order derivative term. For $\delta = 0$, the problem (1.1)-(1.3) is converted into a boundary value problem for the singularly perturbed ordinary differential equation. The reduced problem corresponding to the singularly perturbed differential equation (1.1)-(1.3), obtained by setting $\varepsilon = 0$ in the problem, for $\delta = 0$ is the equation $p(x)y'(x) + q(x)y(x) = f(x)$.

Note that the resolution of the reduced problem satisfy both arbitrary preassigned boundary conditions simultaneously at the boundary points, due to the order of the differential equation will be reduced for one unit. Accordingly, the solution $y(x)$ shows boundary layer, i.e., regions of rapid change in the solution near the one of the end points relying on the sign of $p(x)$. Furthermore, the layer is maintained for $\delta \neq 0$ but sufficiently small.

In this paper, we consider both cases, where the boundary layer is either on the left side or on the right side of the interval [0,1].

It is well known that the standard discretization methods for solving singular perturbation problems are unstable and fail to give accurate results for small values of the perturbation parameter ε. Hence, it is interesting to construct new numerical tolls for this purpose.

During the last decade, researchers have tried to develop a group of meshless or meshfree methods which are based on radial basis function (RBFs) [4, 11, 2]. In particular, the radial basis function collocation method is one of the attractive meshless methods. In 1990, Kansa [9] proposed the use of RBFs for the numerical solution of the Navier-Stokes equations. Since then, RBFs have been used to solve a variety of ordinary and PDEs.

In the present paper, we employ RBFs to solve boundary value problem (1.1)-(1.3). Our solution method is based on an integral formulation of multiquadric collocation. Integration is a smoothing operation, so the convergence rate may be expected to accelerate in line with the convergence rate estimates of Madych and Nelson [14, 16].

Further applications of the RBF integral formulation can be found in Mai-Duy and Tran-Cong [17, 18], and Kansa et al. [10]. When we solve (1.1)-(1.3) with a collocation method, there are a number of difficulties associated in its use. Especially with very small parameter ε, large N is required to obtain accurate solution.

In addition, ill-conditioning of the corresponding differentiation matrices with increasing N frequently causes degradation of the observed precision. For a good resolution of the numerical solution, at least one of the collocation points must lie in the boundary layer. If $\varepsilon \ll 1$ and problem possesses a boundary layer of width $O(\varepsilon)$, then on a uniform grid with $O(N^{-1})$ spacing between the points we need $N = O(\varepsilon^{-1})$, which is not practical in most cases. Therefore, most numerical methods use specially designed grids that contain more points in and around the layer(s). For instance, Miller et al. [19] developed a successful upwind central difference scheme on a piecewise uniform mesh. Gartland [5] and Vulanovič [23] suggested exponentially distributed grid points. The multiquadric (MQ) Radial Basis Function (RBF) interpolation method was developed in 1968 by Iowa State University Geodesist Roland Hardy who described and named the method in a paper [7] that appeared in 1971.

It was not recognized by most of the academic researchers until Franke [3] published a review paper in the evaluation of two-dimensional interpolation methods. The main advantage of this type of approximation is that it works for arbitrary geometry with high dimensions and it does not require a mesh at all.

In this paper, we combine the transformation technique with the MQ integral formulation for solving (1.1)-(1.3). The rest of this paper is organized in what follows. The transformation required to solve such problems is discussed in section 2 while in sections 3-4 are dedicated to the derivation of our main numerical procedure. In section 5, we provide an error estimation. Numerical experiments and results are discussed in section 6-8. Finally, a conclusion of the paper will be drawn in section 9.

2. Transformation

As mentioned in previous section, at least one of the collocation points should lie in the boundary layer. There are some well-developed adaptive methods so that nodes will concentrate near the boundary layers. We seek an efficient way to concentrate nodes in boundary layer. For this purpose, we will apply transformations described in [22].

In [22], authors introduced a sequence of variable transformations so that there are some collocation points within distance ε from the boundaries ± 1 even for $\varepsilon \ll 1$ and $N = O(10)$. Without loss of generality, we assume $[a, b] = [-1, 1]$. For $m \geq 1$ these transformations are $x(\zeta) = g_m(\zeta)$, where

$$g_0(\zeta) = \zeta, \quad g_m(\zeta) = sin\left(\frac{\pi}{2} g_{m-1}(\zeta)\right), \quad m \geq 1. \tag{2.1}$$

As can be seen in Figure 1, the graphs of the transformations are flat towards the end points of the interval. This means that the very thin boundary layer is mapped onto a much wider region. Effectively, collocation points are moved into the thin region.

FIGURE 1. Variable transformation $g_1(\zeta)$, $g_2(\zeta)$, $g_3(\zeta)$ and $g_4(\zeta)$.

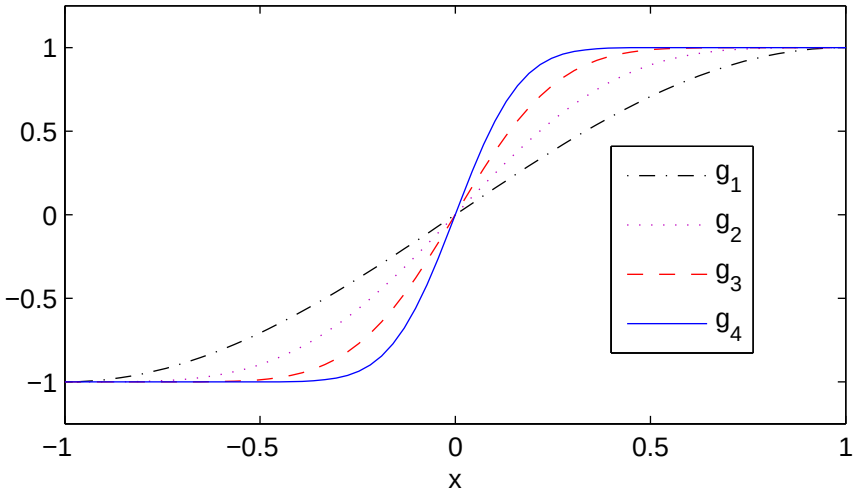

Theorem 2.1. *Let* $\zeta_j = \dfrac{2j}{N} - 1$, $j = 0, 1, \cdots, N$. *The following statement hold for any integer* $m \geq 0$

$$g_m(\zeta_0) - g_m(\zeta_1) = g_m(\zeta_{N-1}) - g_m(\zeta_N) = O(N^{-2^m}). \tag{2.2}$$

Proof. For estsblishing (2.2), first, we prove by induction that $g_m(\zeta_0) - g_m(\zeta_1) = O(N^{-2^m})$.

For $m = 0$, we have $g_0(\zeta_0) - g_0(\zeta_1) = \zeta_0 - \zeta_1 = -1 + (-1 + \dfrac{2}{N}) = -\dfrac{2}{N} = O(N^{-1})$ assume

$$g_k(\zeta_0) - g_k(\zeta_1) = O(N^{-2^k}),$$

thereby, we have

$g_{k+1}(\zeta_0) - g_{k+1}(\zeta_1) = -1 - sin(\dfrac{\pi}{2} g_k(\zeta_1)) = -1 - sin(\dfrac{\pi}{2}(-g_k(\zeta_0) + O(N^{-2^K}))) = O(N^{-2^{K+1}})$.

Since $g_m(\zeta_N) = -g_m(\zeta_0)$ and $g_m(\zeta_{N-1}) = -g_m(\zeta_1)$, the proof of (2.2) is hereby complete. □

Throughout the paper, we refer to x as a physical variable and ζ as a computational variable, the singularly perturbed differential-difference equations (1.1)-(1.3) are transformed into the new BVP

$$\varepsilon v''(\zeta) + P(\zeta)v'(\zeta) + Q(\zeta)v'(\zeta - \delta) + R(\zeta)v(\zeta) = F(\zeta), \quad \forall \zeta \in (0, 1), \tag{2.3}$$

$$v(\zeta) = \omega(\zeta) \quad on - \delta \leq \zeta \leq 0 \tag{2.4}$$

$$v(1) = \gamma, \tag{2.5}$$

Where v is the transplant of y and $v(\zeta) = y(x(\zeta))$. The transformed coefficients are

$$P(\zeta) = \frac{\varepsilon\zeta^{''}(x)}{\zeta^{'}(x)^2}, \qquad Q(\zeta) = \frac{p(x)}{\zeta^{'}(x)},$$

$$R(\zeta) = \frac{q(x)}{\zeta^{'}(x)^2}, \qquad F(\zeta) = \frac{f(x)}{\zeta^{'}(x)^2}.$$

Note that The SINE-transforms (2.1) map the intervals $[-1, 0]$ and $[0, 1]$ onto themselves. Since the BVP (1.1)-(1.3) has only one layer on the left (or right), we translate the physical domain to $[-1, 0]$ (or $[0, 1]$, respectively).

3. An outline of MQ RBF collocation method

3.1. **MQ RBF.** Given a set of N distinct points $\{x_i \in \omega, i = 1, \ldots, N\}$, where ω is a bounded domain in $\mathbb{R}^d$. These points are called centers. A RBF is a function $\Phi(r; c), r = \|x - x_i\|_2$, whose value depends only on the distance from some center points. There are a large class of RBF. The basis function used by Hardy were the quadric surfaces

$$\phi(r; c) = \sqrt{c^2 + r^2}, \tag{3.1}$$

where c is a shape parameter. The RBF (3.1) is called the multiquadric or MQ RBF. It has become common to redefine the MQ (3.1) by first letting $c = \frac{1}{\epsilon}$ and ignoring the scaling factor $\frac{1}{\epsilon}$, which result in

$$\phi(r; \epsilon) = \sqrt{1 + \epsilon^2 r^2}. \tag{3.2}$$

Now, we employ Integrate multiquadric RBF. Integrate RBF methods integrate the original RBF with respect to r, one or more times, to get new basis function in hope of restoring or even improving the convergence of the RBF methods [15]. The notation $\phi^n(r)$ represent an RBF that has been integrated $(n > 0)$ n times with respect to r:

$$\Phi^{''}(r) = \phi(r) = \sqrt{1 + \epsilon^2 r^2},$$

$$\Phi^{'}(r) = \phi^1(r) = \frac{(\epsilon r\sqrt{1 + \epsilon^2 r^2} + sinh^{-1}(\epsilon r))}{2\epsilon},$$

$$\Phi(r) = \phi^2(r) = \frac{(-2 + \epsilon^2 r^2)\sqrt{1 + \epsilon^2 r^2} + 3\epsilon r sinh^{-1}(\epsilon r)}{6\epsilon^2}.$$

The integrated MQ basis functions are referred to as IMQ1 and IMQ2 to indicate how many times they have been integrated. Due to the exponential convergence and superior performance of the IMQ2. Here, the IMQ2 will be used.

3.2. **Collocation method.** Now, we briefly introduce the RBFs collocation method. Let $\Omega \subseteq \mathbb{R}^d$, consider the following boundary value problem (BVP)

$$Lu = f \quad in\, \Omega, \tag{3.3}$$

$$u = g \quad on\, \partial\Omega, \tag{3.4}$$

where L is a linear differential operator and d is the dimension of the problem. For nonlinear operators, some kind of linearization will be needed to seek the solution iteratively. We distinguish in our notation center $X = \{x_1, ..., x_N\}$ and the collocation points $\Xi = \{\alpha_1, ..., \alpha_N\}$. We seek the approximate solution $u\ (x)$ of (3.1) and (3.3) in the form

$$\tilde{u}(x) = \sum_{i=1}^{N} \lambda_i \phi(\|x - x_i\|), \tag{3.5}$$

where λ_i's coefficients to be determined by collocation, ϕ is a radial basis function, $\|.\|$ is the Euclidean norm, and x_i is the center of the radial basis function.

Now, let Ξ be divided into two subsets. One subset contains N_I centers, Ξ_1, where Eq.(3.1) is enforced and the other subset contains N_B centers, Ξ_2, where boundary conditions are enforced.

The collocation matrix that is obtained by matching the differential equation and the boundary condition at the collocation points has the following form

$$A = \begin{bmatrix} A_I \\ A_B \end{bmatrix},$$

where $A_I = L\phi(\|\alpha - x_j\|)_{\alpha=\alpha_i}, \alpha_i \in \Xi_1, x_j \in X$, and $A_B = L\phi(\|\alpha - x_j\|)_{\alpha=\alpha_i}, \alpha_i \in \Xi_2$, $x_j \in X$. The unknown coefficients λ_i are determined by solving the linear system $A\lambda = F$, where F is a vector consisting $f(\alpha_i)$, $\alpha_i \in \Xi_1$, and $g(\alpha_i)$, $\alpha_i \in \Xi_2$.

4. Application of the MQ RBF collocation Method

In this section, we are interested in solving singularly perturbed differential difference equations (2.3)-(2.5) by the MQ RBF collocation method. For this purpose, we rewrite the equations (2.3)-(2.5) as follows:

$$\varepsilon v''(\zeta) + P(\zeta)v'(\zeta) + R(\zeta)v(\zeta) = F(\zeta) - Q(\zeta)\omega'(\zeta - \delta), \quad 0 < \zeta \leq \delta \tag{4.1}$$

$$\varepsilon v''(\zeta) + P(\zeta)v'(\zeta) + Q(\zeta)v'(\zeta - \delta) + R(\zeta)v(\zeta) = F(\zeta), \quad \delta < \zeta < 1 \tag{4.2}$$

$$v(0) = \omega(0); \tag{4.3}$$

$$v(1) = \gamma. \tag{4.4}$$

Now, we choose N equally spaced nodes $\zeta_i, i = 1, 2, \ldots, N$ in computational domain and approximate the unknown function $v(\zeta)$ in equation (4.1)-(4.4) by

$$\tilde{v(\zeta)} = \textstyle\sum_{i=1}^{N} \lambda_i \Phi(\|\zeta - \zeta_i\|) + \gamma_1 + \gamma_2 \zeta,$$

Using collocation method, one obtains the following linear system with N equations and $N+2$ unknowns $\lambda_1, \lambda_2, \ldots, \lambda_N, \gamma_1, \gamma_2$, as follows:

$$\sum_{j=1}^{N}\{\varepsilon\Phi''(r_{ij}) + P(\zeta_i)\Phi'(r_{ij}) + R(\zeta_i)\Phi(r_{ij})\}\lambda_j + R(\zeta_i)\gamma_1 + (R(\zeta_i)\zeta_i + P(\zeta_i))\gamma_2 = F(\zeta_i) - Q(\zeta_i)\omega'(\zeta_i - \delta), \quad 0 < \zeta_i \leq \delta, \tag{4.5}$$

$$\sum_{j=1}^{N}\{\varepsilon\Phi''(r_{ij}) + P(\zeta_i)\Phi'(r_{ij}) + Q(\zeta_i)\Phi'(\|\zeta_i - \delta - \zeta_j\|) + R(\zeta_i)\Phi(r_{ij})\}\lambda_j + R(\zeta_i)\gamma_1 + (P(\zeta_i) + Q(\zeta_i) + R(\zeta_i)\zeta_i)\gamma_2 = F(\zeta_i), \quad \delta < \zeta_i < 1, \tag{4.6}$$

$$\sum_{j=1}^{N}\lambda_j\Phi(r_{1j}) + \gamma_1 + \gamma_2\zeta_1 = \omega(\zeta_1), \quad \zeta_1 = 0,$$

$$\sum_{j=1}^{N}\lambda_j\Phi(r_{Nj}) + \gamma_1 + \gamma_2\zeta_N = \gamma, \quad \zeta_N = 1,$$

where $r_{ij} = \|\zeta_i - \zeta_j\|$. We impose two supplementary collocation conditions at ζ_1 and ζ_N in (4.1) and (4.2), respectively, to obtain a $(N+2)\times(N+2)$ system of linear equations.
We have used the Gaussian elimination method to solve such a system.
Note that this provides the solution in the form of a function that can be evaluated anywhere in $[0,1]$ and no additional interpolation is required.

5. Error estimation

Let us call $e(\zeta) = v(\zeta) - \tilde{v}(\zeta)$ as the error function. Where $v(\zeta)$ is the exact solution of (2.3)-(2.5) and $\tilde{v}(\zeta)$ is approximation of $v(\zeta)$. Hence,

$$\varepsilon\tilde{v''}(\zeta) + P(\zeta)\tilde{v'}(\zeta) + Q(\zeta)\tilde{v'}(\zeta - \delta) + R(\zeta)\tilde{v}(\zeta) - F(\zeta) = R(\zeta), \ \forall\zeta \in (0,1), \tag{5.1}$$

$$\tilde{v}(\zeta) - \omega(\zeta) = R_1(\zeta), \quad -\delta \leq \zeta \leq 0, \tag{5.2}$$

$$\tilde{v}(\zeta) - \gamma = R_2(\zeta), \quad \zeta = 1, \tag{5.3}$$

and

$$\varepsilon v''(\zeta) + P(\zeta)v'(\zeta) + Q(\zeta)v'(\zeta - \delta) + R(\zeta)v(\zeta) - F(\zeta) = 0, \ \forall\zeta \in (0,1), \tag{5.4}$$

$$v(\zeta) - \omega(\zeta) = 0, \quad -\delta \leq \zeta \leq 0, \tag{5.5}$$

$$v(1) - \gamma = 0. \tag{5.6}$$

By subtracting Eqs. (5.4)-(5.6) from (5.1)-(5.3), we have

$$\varepsilon(v''(\zeta) - \tilde{v}(\zeta)) + P(\zeta)(v'(\zeta) - \tilde{v}'(\zeta)) + Q(\zeta)(v'(\zeta - \delta) - \tilde{v'}(\zeta - \delta)$$

$$+R(\zeta)(v(\zeta)-\tilde{v}(\zeta))=-R(\zeta),\ \ o<\zeta<1,$$
$$v(\zeta)-\tilde{v}(\zeta)=-R_1(\zeta),\qquad -\delta\le\zeta\le 0,$$
$$v(1)-\tilde{v}(1)=-R_2(\zeta),\qquad \zeta=1.$$

Now, the error function $e(\zeta)$ is satisfying below problem

$$\varepsilon e''(\zeta)+P(\zeta)e'(\zeta)+Q(\zeta)e'(\zeta-\delta)+R(\zeta)e(\zeta)=-R(\zeta),\qquad 0<\zeta<1,$$
$$e(\zeta)=-R_1(\zeta),\qquad -\delta\le\zeta\le 0,$$
$$e(\zeta)=-R_2(\zeta),\qquad \zeta=1.$$

Since the function $R(\zeta)$ is known, so to find approximate error, we follow the same method mentioned in section 4.

6. Numerical experiments

This section is devoted to the computational results. We present the numerical results of proposed method on several test problems with right and left layer. The unknown function $v(\zeta)$ in the transformed BVP (2.3) is approximated with $v(\zeta)=\sum_{i=1}^{N}\lambda_i\Phi(\|\zeta-\zeta_i\|)+\gamma_1+\gamma_2\zeta$, where Φ is IMQ2 basis function.

The accuracy of the RBFs solution, depends heavily on the choice of a parameter c in radial basis function. We use uniformly distributed data center for all examples and shape parameter $c_j=0.815d_j$ for the IMQ2 basis, suggested in [7], where d_j is the distance from j^{th} point to its nearest neighbor, a constant shape parameter for uniformly distributed data center.

All codes were written in **MatlabR2012a** on a 2.30 MHz Alpha Machine with 4 GB RAM. Since the exact solutions are not known for the considered examples, we use two ways for reporting the errors as follows
i) double mesh principle $E_{\varepsilon}^{N}=\max|y_i^N-y_{2i}^{2N}|$.
ii) residual error $E_r^N=|L(y_i^N)-f(x_i)|$,
where x_i does not belonging to the collocation points in residual error. We remark that some of the data points in the physical domain coincide numerically near the boundaries. This does not cause difficulties, as there is no coincidence in the computational domain.

Example 6.1. First, we consider the following BVP

$$\varepsilon y''(x)+y'(x-\delta)-y(x)=0,\ \ \forall x\in(0,1),\tag{6.1}$$

$$y(x)=1\ \ \text{on}\ \ -\delta\le x\le 0,\tag{6.2}$$

$$y(1)=1,\tag{6.3}$$

the transformed equations with new variable $\zeta=\zeta(x)$ are

$$\varepsilon v''(\zeta)+\frac{\varepsilon\zeta''(x)}{\zeta'(x)^2}v'(\zeta)+\frac{1}{\zeta'(x)}v'(\zeta-\delta)-\frac{1}{\zeta'(x)^2}v(\zeta)=0,\ \ \forall\zeta\in(0,1),\tag{6.4}$$

$$v(\zeta)=1\ \ \text{on}\ \ -\delta\le\zeta\le 0,\tag{6.5}$$

$$v(1) = 1. \tag{6.6}$$

FIGURE 2. Solution of Example 6.1 plotted against the computational variable and physical variable.

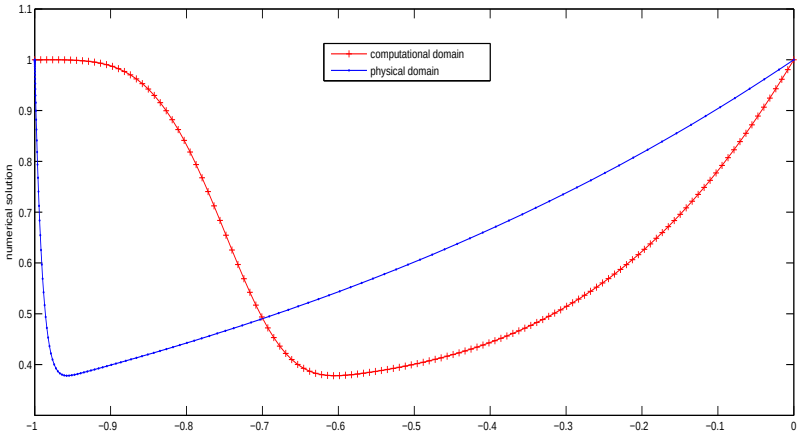

FIGURE 3. Numerical Solution for Example 6.1, $m = 2$, $N = 128$, $\epsilon = 0.01$.

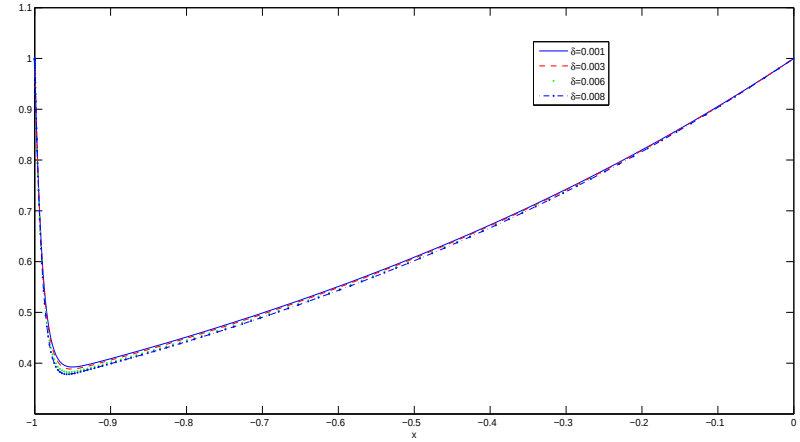

FIGURE 4. The numerical solution of Example 6.1, $\varepsilon = 0.01, m = 0$

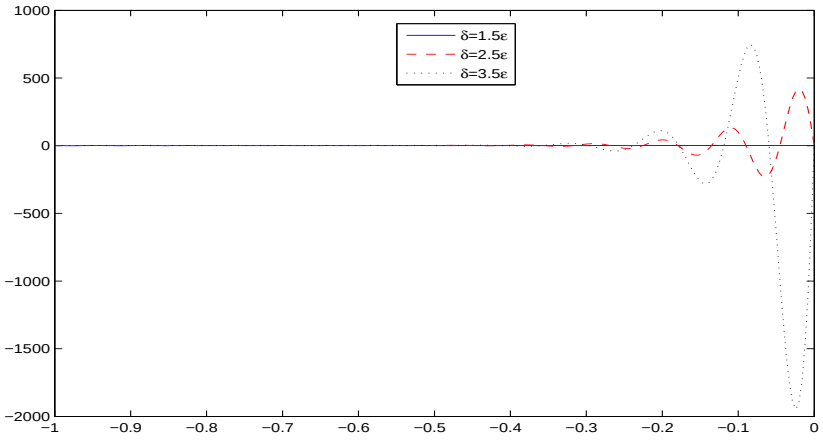

FIGURE 5. The numerical solution of Example 6.1, $\varepsilon = 0.01, m = 0$

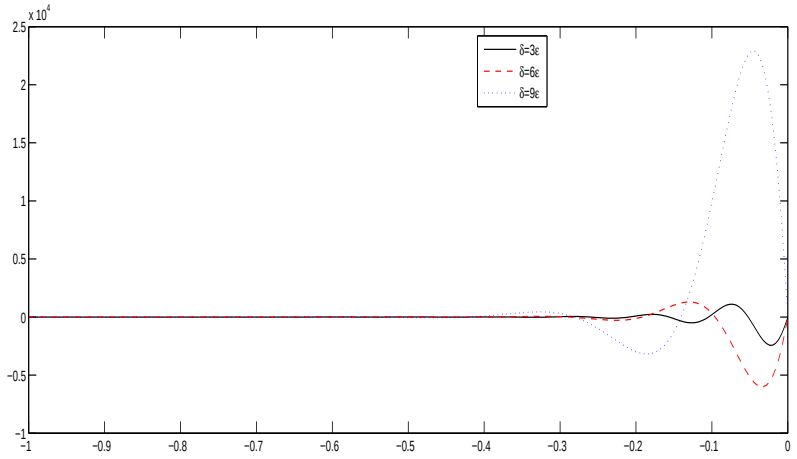

FIGURE 6. Maximum Residual Error for Example 6.1 with $\delta = 0.008$, $\epsilon = 0.01$, as a function of N.

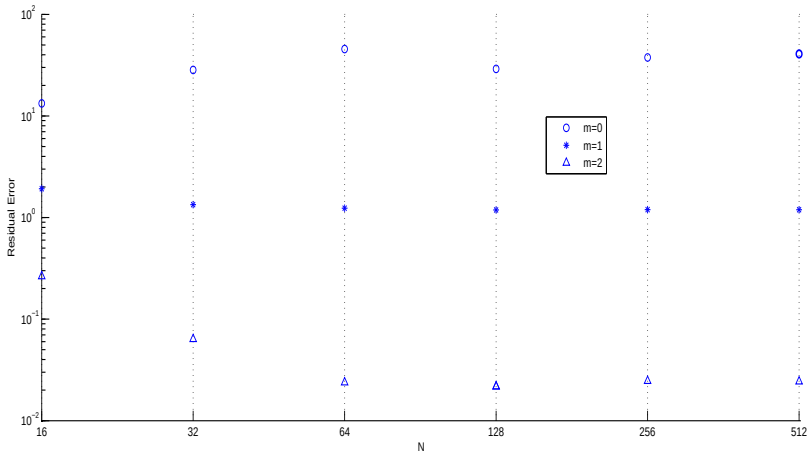

Example 6.2. Now, we consider BVP (1.1)-(1.3) with variable coefficients, i.e., for $p(x) = e^{-0.5x}$, $q(x) = -1$, $f(x) = 0$, $\omega(x) = 1$ and $\gamma = 1$.

FIGURE 7. Graph of the numerical solution of Example 6.2, $m = 2$, $N = 128$, $\varepsilon = 0.01$.

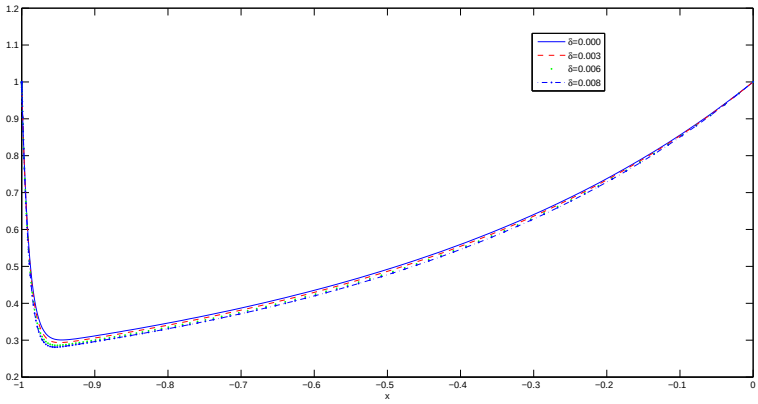

FIGURE 8. Maximum Residual Error for Example 6.2 with $\delta = 0.00003$, $\epsilon = 0.0001$, as a function of N.

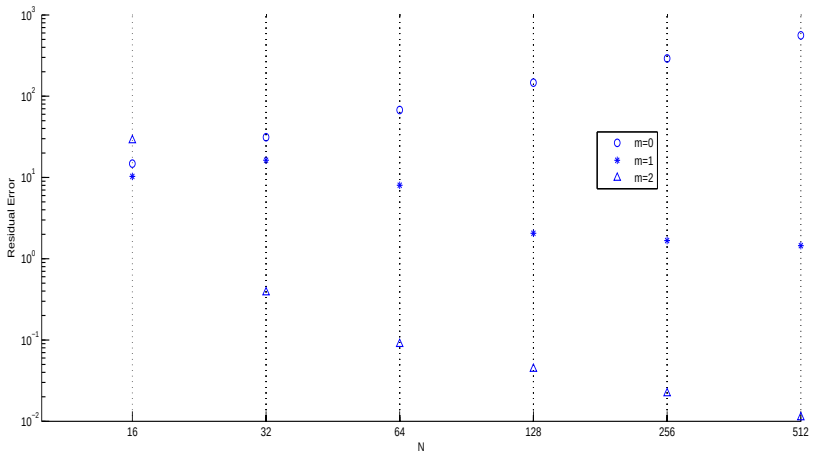

Example 6.3. To demonstrate the efficiency in the case when boundary layer occurs on the right side, we consider the BVP (1.1)-(1.3) with constant coefficients, i.e., for $p(x) = -1$, $q(x) = -1$, $f(x) = 0$, $\omega(x) = 1$ and $\gamma = -1$.

We have plotted the graphs of computed solution of the problems for a set of 128 uniform centers, $m = 2$ and for different values of δ and ε , in Figures 3, 7 and 9. As Figure 3 shows, the BVP (6.1)-(6.3) has one boundary layer on the left side of the underlying interval and as Figure 9 shows, the BVP in example 6.3 has one right boundary layer.

We observe that if $\delta = o(\varepsilon)$, the layer behavior is maintained in both the cases (i.e., the left side boundary layer case and the right boundary layer case) whether the coefficient of the delay term is of O(1) or o(1).

As the delay increases, the thickness of the layer decreases in the case when the solution exhabits layer behavior on the left side as shown in Figures 3 and 7. While in the case of the right side boundary layer, it increases as shown in Figures 9 and 10.

If $\delta = O(\varepsilon)$, in the case of the left side boundary layer, the layer behavior of the solution is no longer maintained whether the coefficient of the delay term is of O(1) or o(1) and the solution exhabits oscillatory behavior. Not only the layer behavior is destroyed oscillations previosly confined to the layer region are extended across the entire interval [0,1] also as shown in Figures 4 and 5. While in the case of the right side boundary layer, the layer behavior of the solution is maintained although the coefficent of the delay term is of o(1) as shown in Figure 10.

Figures 6, 8 and 12 show residual error for different values of δ and ε as a function of N. We observe as m increases the residual error decreases. Tables 1-3 give the maximum error for different δ, m and N for the above examples. We observe in tables 1-3 as SINE-transforms increase the maximum error decreases.

The reader can see the results we get using integrated multiquadric collocation method

are much better than the results are given in [8].
Note: we have used SINE transforms, only the solution has the boundary layer behavior. When the solution has oscillatory behavior, employing SINE transforms does not improve the accuracy of the solution. Even, it may decrease the accuracy.

FIGURE 9. Graph of the numerical solution of Example 6.3, $m = 2$, $N = 128$, $\varepsilon = 0.001$.

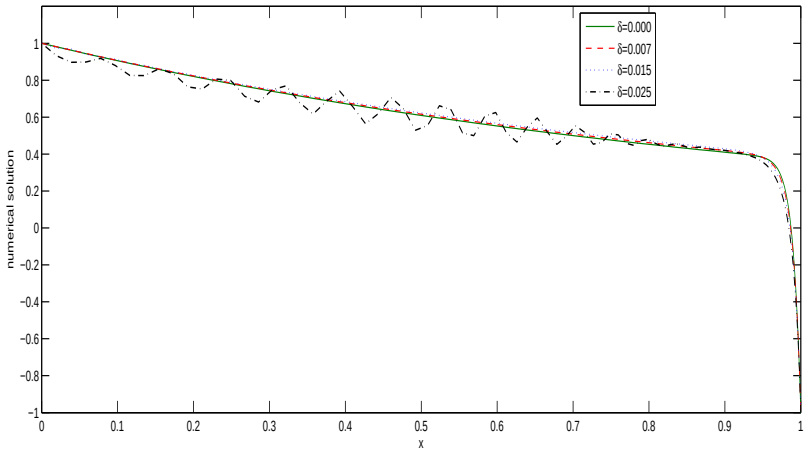

FIGURE 10. The numerical solution of Example 6.3, $\varepsilon = 0.01$, $m = 0$.

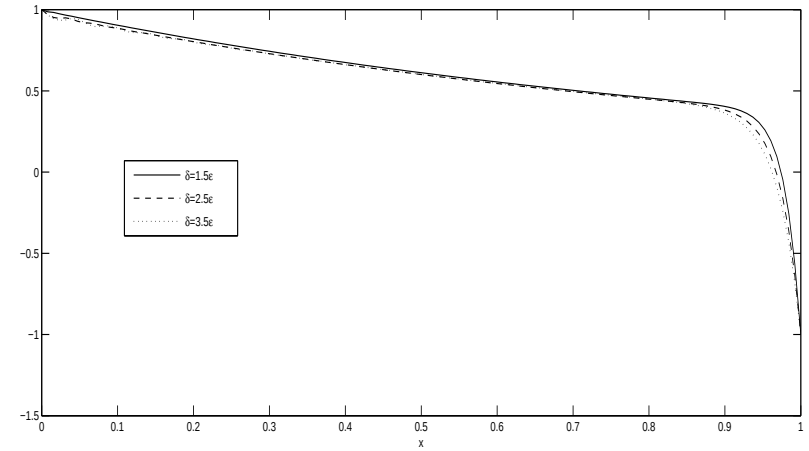

FIGURE 11. The numerical solution of Example 6.3, $\varepsilon = 0.01$, $m = 0$.

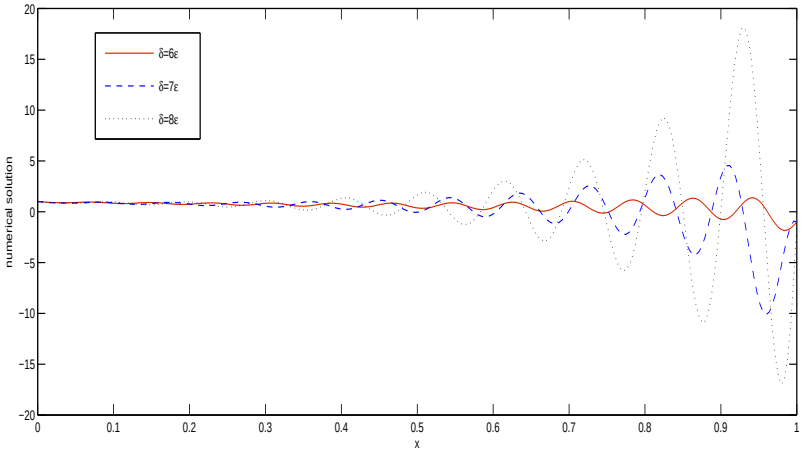

FIGURE 12. Maximum Residual Error for Example 6.3 with $\delta = 0.0007$, $\epsilon = 0.001$, as a function of N.

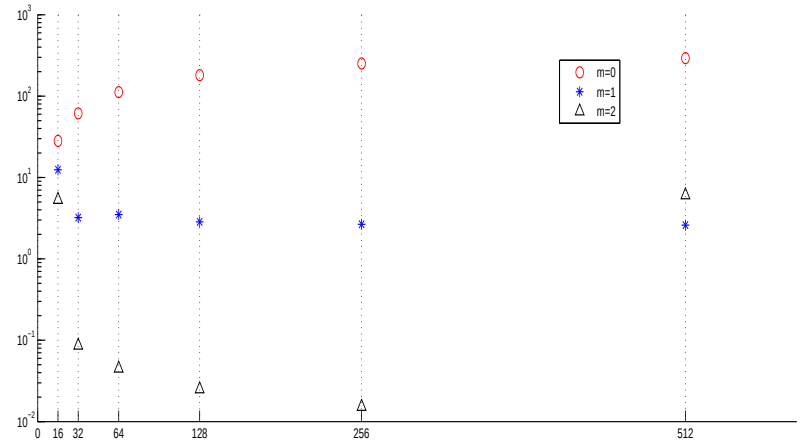

TABLE 1. Maximum error of Example 6.1 for $\varepsilon = 0.1$.

δ	$\frac{N}{M}$	50	100	150	200
	0	0.0016	0.0018	0.0011	$7.8027e-04$
0.01	1	$4.0293e-04$	$1.0051e-04$	$4.0771e-05$	$2.4045e-05$
	2	$1.0594e-04$	$2.4423e-05$	$1.1186e-05$	$6.3543e-06$
	0	0.0094	0.0051	$4.0667e-05$	0.0025
0.03	1	$3.4102e-04$	$1.1078e-04$	$4.0667e-05$	$3.4171e-05$
	2	$3.4797e-04$	$2.5754e-05$	$1.1517e-05$	$6.4644e-06$
	0	0.0263	$2.7909e-04$	0.0083	0.0062
0.08	1	$7.2511e-04$	$2.7909e-04$	$1.6780e-04$	$1.1895e-04$
	2	$5.5385e-04$	$1.3903e-04$	$6.2231e-05$	$3.5168e-05$

TABLE 2. Maximum error for Example 6.2 for $\varepsilon = 0.01$.

δ	$\frac{N}{M}$	50	100	150	200
	0	0.0081	0.0142	0.0100	0.0069
0.001	1	0.0048	0.0011	$5.0165e-04$	$2.8042e-04$
	2	$6.5852e-04$	$1.4348e-04$	$5.8195e-05$	$3.0685e-05$
	0	0.008560	0.0237	0.0195	$2.8459e-04$
0.003	1	0.0048	0.0011	$5.0323e-04$	$2.8459e-04$
	2	$6.9742e-04$	$1.4210e-04$	$5.2190e-05$	$2.5779e-05$
	0	0.0561	0.3728	0.0675	0.0723
0.008	1	0.0561	0.0012	$4.7590e-04$	$2.8209e-04$
	2	$7.0626e-04$	$8.6747e-05$	$4.1835e-05$	$2.6218e-05$

TABLE 3. Maximum error for Example 6.3 for $\varepsilon = 0.001$.

δ	$\frac{N}{M}$	50	100	150	200
	0	0.281446	0.1355	0.0520	0.0200
0.0007	1	0.0808	0.0227	0.0099	0.0055
	2	$3.0191e-04$	$5.4816e-05$	$2.3388e-05$	$1.2601e-05$
	0	0.2075	0.0566	0.0129	0.0382
0.0015	1	0.0802	0.0229	0.0100	0.0055
	2	$3.0193e-04$	$5.1258e-05$	$2.0834e-05$	$1.0483e-05$
	0	0.1367	0.0165	0.0498	0.0634
0.0025	1	0.0794	0.0231	0100	0056
	2	$3.0195e-04$	$4.5959e-05$	$1.6214e-05$	$5.8972e-06$

7. Conclusion

In this paper, an effective method is proposed for solving singularly perturbed differential-difference equations with boundary layer. The present method is based on coordinate stretching transform and the integrated multiquadric (MQ) collocation method. Numerical results show that the presented method is an accurate and reliable technique for singularly perturbed differential-difference equations with boundary layer.

Acknowledgment

This research was supported by a grant from Ferdowsi University of Mashhad No.3/28880, the authors would like to express their deep appreciation to the editor and referees for their comments and suggestions.

References

[1] M. W. Derstine, H. M. Gibbs, F. A. Hopf, and D. L. Kaplan, *Bifurcation gap in a hybrid optical system*, Phys. Rev. A, 26, 3720(R).

[2] M. Elansari, D. Ouazar, and H. D. Cheng, *Boundary solution of Poisson's equation using radial basis function collocated on Gaussian quadrature nodes*, Commun. Numer. Meth. Eng., *17*(7) (2001), 455-464.

[3] R. Franke, *Scattered data interpolation: test of some methods*, Math. Comput., *38* (1982), 181-200.

[4] C. Franke and R. Schaback, *Solving partial differential equations by collocation using radial basis functions*, Appl. Math. Comp., *93* (1998), 73-82.

[5] E. C. Gartland, *Graded-mesh difference schemes for singularly perturbed two-point boundary value problems*, Math. Comput., *51* (1995), 631-657.

[6] V. Y. Glizer, *Asymptotic analysis and solution of a finite-horizon H1 control problem for singularly-perturbed linear systems with small state delay*, J. Optim. Theory Appl., *117* (2003), 295-325.

[7] R. L. Hardy, *Multiquadric equations of topography and other irregular surfaces*, J. Geophys. Res., *176* (1971), 1905-1915.

[8] M. K. Kadalbajoo and K. K. Sharma, *Numerical analysis of singularly perturbed delay differential equations with layer behavior*, Appl. Math. Comput., *157* (2004), 11-28.

[9] E. J. Kansa, *Multiquadrics-a scattered data approximation scheme with applications to computational fluid-dynamics*, Comput. Math. Appl., *19* (1990), 127-145.

[10] E. J. Kansa, H. Power, G. E. Fasshauer, and L. Ling, *A volumetric integral radial basis function method for time dependent partial differential equations: I. Formulation*, Eng. Anal. Bound. Elem., *28*(10) (2004), 1191-1206.

[11] E. Larsson and B. Fornberg, *A numerical study of some radial basis function based solution methods for elliptic PDEs*, Comput. Math. Appl., *46* (2003), 891-902.

[12] A. Longtin and J. Milton, *Complex oscilations in the human pupil light reflex with mixed and delayed feedback*, Math. Biosci., *90* (1988), 183-199.

[13] M. C. Mackey, *G. L., Oscillations and chaos in physiological control systems, Science*, *197* (1977), 287-289.

[14] W. R. Madych and S. A. Nelson, *Multivariate interpolation and conditionally positive definite functions*, Aprox. Theory Appl., *4* (1988), 77-89.

[15] W. R. Madych and S. A. Nelson, *Multivariate interpolation and conditionally positive definite functions ii*, Math. Comput., *4*(189) (1990), 211-230.

[16] W. R. Madych, *Miscellanrous error bounds for multiquadric and related interpolators*, Comput. Math. Appl., *24*(12) (1992), 121-138.

[17] N. Mai-Duy and T. Tran-Cong, *Numerical solution of Navier-Stokes equations using multiquadric radial basis function networks*, Int. J. Num. Meth. Fluid, *37* (2001), 65-86.
[18] N. Mai-Duy and T. Tran-Cong, *Numerical solution of differential equations using multiquadric radial basis function networks*, Neural Networks, *14* (2001), 185-199.
[19] J. J. H. Miller, E. O'Riordan, and G. I. Shishkin, *On piecewise-uniform meshes for upwind- and central-difference operetors for solving singularly perturbed problems*, IMA J. Numer. Anal., *15*(1) (1995), 89-99.
[20] K. Phaneendra, Y. N. Reddy, and GBSL. Soujanya, *A seventh order numerical method for singular perturbed differential-difference equations with negative shift*, Nonlinear Anal. Model. Control, *16*(2) (2011), 206-219.
[21] R. B. Stein, *A theoretical analysis of neuronal variability*, Biophys. J., *5* (1965), 173-194.
[22] T. Tang and M. R. Trummer, *Boundary layer resolving pseudospectral methods for singular perturbation problems*, SIAM J. Sci. Comput., *17*(2) (1996), 430-438.
[23] R. Vulanovic, *On a numerical solution of a type of singularly perturbed boundary value problem by using a special discretization mesh*, Univ. u Novom Sadu Zb. Rad. Prirod. Mat. Fak. Ser. Mat., *13* (1983), 187-201.
[24] M. Wazewska-Czyzewska and A. Lasota, *Mathematical models of the red cell system*, Mat. Stos., *6* (1976), 25-40.